

**Investigation of bovine bone by resonant ultrasound spectroscopy and
transmission ultrasound**

T. Lee*, R. S. Lakes§, A. Lal¶

*Orthopedic Biomechanics Laboratory
Beth Israel Deaconess Medical Center
Harvard Medical School

330 Brookline Avenue, RN 115, Boston, MA 02215

¶ Department of Biomedical Engineering

§ Department of Engineering Physics, § Engineering Mechanics Program;

§ Materials Science Program and § Rheology Research Center
and

¶ Department of Electrical and Computer Engineering

University of Wisconsin-Madison
147 Engineering Research Building
1500 Engineering Drive, Madison, WI 53706-1687

Address correspondence to R. S. Lakes

Lakes e-mail- lakes@engr.wisc.edu

Office phone (608) 265-8697; fax: (608) 263-7451

Biomechanics and Modeling in Mechanobiology, 1 (2), 165-175 (2002)

ABSTRACT

The method of resonant ultrasonic spectroscopy (RUS) was evaluated for bovine bone and compared with the traditional wave transmission ultrasound method. In RUS, the resonance structure of a cubical or rectangular specimen is scanned. For some low-damping materials a single measurement yields sufficient resonant frequencies to determine all of the anisotropic elastic constants. Bone has a high viscoelastic damping at ultrasonic frequency. Consequently resonance peaks of a cubical specimen tend to overlap. Therefore the usual RUS method must be modified for application to bone; even so one cannot obtain all the elastic constants. Concurrent studies with transmission ultrasound were conducted. Results were used to generate a map of the elastic moduli versus position along the bone axis. Stiffness was greatest in the mid part of the bovine femur.

I. INTRODUCTION

Ultrasonic techniques have been used extensively to explore the anisotropy of bone (Lang 1970; Abendschein and Hyatt 1970; Yoon and Katz 1976; Lees et al. 1979), its composite microelastic character (Lakes et al., 1983), its viscoelastic properties via wave attenuation (Lakes et al. 1986), and its in-vivo properties (Brown and Mayor 1976; Lakes and Saha 1978; Andre et al. 1980). Ultrasonic methods are attractive in that material properties of bone can be obtained non-destructively. One drawback, given that bone properties depend upon deformation rate (Sedlin and Hirsch 1966), is that the frequencies used substantially exceed frequencies associated with locomotion. Wave transmission ultrasound (Fig. 1a) is capable of revealing all of the anisotropic elastic constants of a material. These measurements are painstaking since they involve transmitting waves of different polarization in different directions through specimens. For a full characterization of properties, it is also necessary to study oblique cut specimens.

Resonant ultrasound spectroscopy (RUS, Fig. 1b) is a recent technique which involves scanning the resonance structure of a compact specimen such as cube, parallelepiped, or short cylinder (Maynard 1996; Leisure and Willis 1997). The resonant structure, from about 50 kHz to more than 10 MHz depending on the specimen size, is complex, however advances in computation capacity have enabled the back-calculation of material properties from the resonance frequencies. With the proper configuration and specimen material, a single measurement yields enough frequencies to determine all of the elastic constants for the material (as many as 21 for a crystal with low symmetry) (Migliori and Sarrao 1997). Samples may be prepared in rectangular, spherical or a wide variety of other shapes, and crystalline samples need not be oriented with respect to their crystallographic axes. RUS is also capable of determining mechanical damping of materials (Lee and Lakes 2000).

Mechanical damping, expressed as $\tan \delta$, is the ratio of energy dissipated to energy stored in a cycle of deformation in a linearly viscoelastic material such as bone. Here δ is the phase angle between stress and strain. $\tan \delta$ is the ratio of the imaginary to the real part of the complex modulus. Mechanical damping is important as a probe of energy absorption in both soft and hard living tissues. The damping of human bone attains a minimum of about 0.01 at frequencies from 1 to 100 Hz. The damping increases gradually at both higher and lower frequencies (Lakes 2001). Study of the mechanical damping of wet and dry bovine bone was done using broadband viscoelastic spectroscopy (BVS) (Garner et al. 2000).

The purpose of this study is to evaluate the applicability of RUS to the determination of bone elastic and viscoelastic properties. To that end, a set of cubical specimens from different positions along the length of a bovine femur was prepared. The modulus values obtained from RUS and transmission ultrasound were mapped as a function of position along the bone axis. It was hypothesized based on an interpretation of bone remodeling, that the moduli would be greatest in the midshaft of the bone.

II. ANISOTROPIC PROPERTIES: MEASUREMENT

Ultrasonic methods are capable of determining all the elastic moduli C_{ijkl} of an anisotropic elastic material. RUS can extract these moduli from a single scan of (sufficiently sharp) resonances of a single specimen. Transmission ultrasound requires multiple specimens and several types of transducer.

The modulus tensor C_{ijkl} describes the relationship between stress (σ_{ij}) and strain (ϵ_{kl}) of linearly elastic materials in 3-dimensions:

$$\sigma_{ij} = C_{ijkl} \epsilon_{kl}, \quad (1)$$

where indices i, j, k and l are from 1 to 3 representing x, y and z coordinates; summation is implied over repeated indices. For the fully anisotropic case, there are 81 components for the modulus tensor of which at most 21 are independent. Materials which have some structural symmetry are described by fewer anisotropic elastic constants. For example, orthotropic materials, i.e. wood and bovine bone, with three perpendicular planes of symmetry are described by 9 independent constants as in Eq. 2. The modulus tensor elements are represented (the symbol \Rightarrow) using a reduced index notation (e.g. $C_{44} = C_{2323}$, $C_{55} = C_{1313}$ and $C_{66} = C_{1212}$):

$$C_{ijkl} \Rightarrow \begin{pmatrix} C_{11} & C_{12} & C_{13} & 0 & 0 & 0 \\ C_{12} & C_{22} & C_{23} & 0 & 0 & 0 \\ C_{13} & C_{23} & C_{33} & 0 & 0 & 0 \\ 0 & 0 & 0 & C_{44} & 0 & 0 \\ 0 & 0 & 0 & 0 & C_{55} & 0 \\ 0 & 0 & 0 & 0 & 0 & C_{66} \end{pmatrix} . \quad (2)$$

Here, C_{11} , C_{22} and C_{33} represent axial stiffness in radial, circumferential and longitudinal directions, and C_{44} , C_{55} and C_{66} represent shear moduli. C_{12} , C_{13} and C_{23} are Poisson's ratio related stiffness elements. An axisymmetric material, such as human bone, which appears the same under an arbitrary rotation about an axis, is described by 5 constants. This symmetry is also referred to as transverse isotropy or quasihexagonal symmetry in which C_{22} is equal to C_{11} because of the equivalence of two transverse directions.

These anisotropic elastic constants can be extracted from ultrasonic velocity measurements. The velocity of a longitudinal ultrasonic wave through a material is dependent on the axial stiffness and its mass density for an anisotropic material (Papadakis 1976),

$$V = \sqrt{\frac{C}{\rho}} , \quad (3)$$

in which V is the velocity, C is the modulus tensor element associated with the particular kind of wave, and ρ is the mass density. From the compressional wave velocities of ultrasound and from the density of bone, the axial moduli for radial (C_{11}), circumferential (C_{22}) and longitudinal (C_{33}) directions can be calculated. These are tensorial moduli, not Young's moduli. The distinction arises since the wavelength of the ultrasonic waves is considerably smaller than the specimen dimensions, so the Poisson effect is largely suppressed. Shear moduli C_{44} , C_{55} and C_{66} can be found from shear wave velocity studies using shear transducers. Mechanical damping, $\tan \delta$, can be extracted from wave attenuation measurements (not done in the present study).

Most of the natural frequencies of a vibrating cube used in RUS, even an isotropic one, are not amenable to solution by analytical means. However, following Demarest (1971), the lowest mode in an isotropic cube has an analytical solution and is a torsional mode,

$$f = \frac{\sqrt{2}}{L} \sqrt{G} , \quad (4)$$

with G as the shear modulus, ρ as density and L as the length of a cube side. Demarest used numerical methods to determine the natural frequencies of the remaining modes which are shown in Fig. 2. The lowest mode is clearly distinguishable in Fig. 2 because the torsional frequency is far from the others. Fig 2 illustrates the complexity of the mode structure in the isotropic case. For anisotropic materials such as bone, the structure of the higher modes would be even more complex. Higher modes are closer together; even so, the peaks are well defined since they are sharp, provided $\tan \delta$ is sufficiently small. In standard RUS testing, a scan of resonant frequencies is performed,

and a computer based numerical algorithm is applied to extract the anisotropic elastic constants from the spectrum, the known density, and the dimensions of the specimen. In the present studies of bone, viscoelasticity gave rise to resonant peaks which were sufficiently broad that they overlapped. This prevented numerical inversion by the RUS software.

Mechanical damping, $\tan \delta$, can be extracted from experimental resonant data from RUS or other techniques by fitting an exact analytical expression to the curve of resonant amplitude versus frequency. For a small $\tan \delta$, one may use several approximation schemes to infer damping from a peak of the resonance curve. For example, in the half-width approach, the dynamic compliance is determined at a resonance; then the oscillator is tuned until the response is half the value at resonance (Lakes 1998). The damping is given by

$$\tan \delta = \frac{1}{\sqrt{3}} \frac{\Delta \omega}{\omega_0}, \quad (5)$$

in which ω_0 is the angular frequency at a resonance. The $\Delta \omega$ represents the full width of the resonance curve at half maximum amplitude. The relative width of the resonance curve is referred to as Q^{-1} with Q as the "quality factor", a term also used in describing resonant behavior in other systems including electric circuits. For $\tan \delta < 0.2$, $\tan \delta \approx Q^{-1}$ (Graesser and Wong 1992).

One may also fit the resonance data to a Lorentzian function to obtain the mechanical damping ($\tan \delta$) as follows. For a lumped system with a large attached inertia, the normalized dynamic torsional compliance is (Koppellmann 1958):

$$C = \frac{1}{\sqrt{[1 - (\omega / \omega_0)^2]^2 + \tan^2 \delta}}, \quad (6)$$

in which $\tan \delta$ is the loss tangent, a measure of mechanical damping and ω_0 is the natural frequency. The dependence of C on frequency is referred to as a Lorentzian function, sometimes called as a Lorentzian line shape, in view of the form of the spectral lines associated with electromagnetic radiation (light) from atomic resonances. The Lorentzian is also a good approximation of the lowest torsion resonant peak of a distributed system (Lee and Lakes 2000).

III. EXPERIMENTAL METHODS

Specimens

Cubic-shaped bone specimens were prepared for use in both using RUS experiments and through transmission ultrasonic experiments. A bovine femur was obtained from a (female) Holstein cow, 2 years old, and 1200 lbs. The femur is a large bone which permits study of many relatively large specimens from the same bone. The bone was maintained fresh in a cooler. It was 48 cm long and cut into 18 pieces after removing the femoral head and knee condyles (Fig. 3). Bone specimens were then frozen with Ringer's solution in individually sealed plastic bags until

they were thawed for machining. Freezing appears not to affect mechanical properties of bone significantly (Hamer et al. 1996). Specimens were rough cut into a cubic shape (approximately 1 cm³) with a band saw, then fine cut with a diamond saw (Isomet low speed saw, Buehler) while moist with Ringer's solution. The anterior cube face was identified by a green spot of acrylic paint and a spot on the proximal face was painted yellow for orientation. The mass of each specimen was determined and its density calculated. All specimens were refrigerated and kept wet in Ringer's solution between tests. During tests they were at room temperature (~22°C) and were kept wet with drip. Since overlap of fundamental mode peaks observed in cubical specimens obtruded in interpretation of results, an additional rectangular parallelepiped specimen was prepared to split the fundamental torsion peak. To that end, a rectangular sample with 20% ratio between the dimensions (1 : 0.8 : 0.64) was prepared using a diamond saw as in the case of a cube sample

Resonant ultrasound spectroscopy (RUS)

Testing

The RUS system is made by Dynamic Resonance Systems, (255 Lane 13, Powell, WY 82435), Model DRS modulus I. It consists of two data processing boards and one set of PZT (Lead Zirconate Titanate) transducers. Each transducer has a face diameter of 4 mm and length of 3 mm. Each specimen was mounted by its corners, and offset from its center, between the transducers, as shown in Fig. 1 (b). The transducers are mounted on spring loaded adjustable plastic arms. Anisotropic bone samples were placed with careful reference to their symmetry axes: the bone's longitudinal, circumferential, and radial directions. Frequency scanning and data processing were done using software developed by DRS Inc. in an IBM Pentium PC connected to the RUS system. The real and imaginary parts of the signal were saved and exported. Data were plotted using Kaleidagraph graphic software and a Lorentzian function was fitted to selected resonant peaks for inference of damping. Resonant frequencies were determined several times.

In the RUS scanning, noise was observed near 127 kHz and 170 kHz. Many experimental trials were made to determine the cause of the peak by changing contact points, rotating the sample, and trying other specimens. System noise occurred in every test independent of operating conditions. A further peak near 100 kHz, notable in tests of small specimens was evaluated as follows. RUS transducers were placed 5 mm apart with no sample. Another spectrum was taken. The test was repeated with a piece of paper in between, but not touching, the transducers. A peak in the voltage amplitude was obtained around 100 kHz for both cases, but the amplitude with the paper was a factor of ten smaller than the air alone. This implies that this peak was caused by the resonance of the air.

Analysis

To choose a range of frequencies of scanning, baseline values for bone properties were considered as follows. Three shear moduli from prior ultrasonic tests (Van Buskirk and Ashman 1981, Table 1) were assumed initially to obtain effective shear moduli which govern torsional rigidity of a bar (Gere and Timoshenko 1990; Lekhnitskii 1977). Effective shear moduli are expressed in terms of the tensorial shear moduli, C_{44} , C_{55} and C_{66} , as follows.

$$G_{\text{eff1}} = \frac{2}{\frac{1}{C_{55}} + \frac{1}{C_{66}}} \quad G_{\text{eff2}} = \frac{2}{\frac{1}{C_{44}} + \frac{1}{C_{66}}} \quad G_{\text{eff3}} = \frac{2}{\frac{1}{C_{44}} + \frac{1}{C_{55}}} \quad . \quad (7)$$

The calculated effective shear modulus was input to Eq. 4 to determine the frequency range over which RUS experiments were to be conducted upon a cube of wet bovine bone.

Since a RUS based numerical computation of the full set of elastic constants was not feasible, an alternate approach to the determination of only the three principal shear moduli was explored. According to Lekhnitskii (1977), the generalized torsional rigidity of a bar of rectangular section can be formulated in an infinite series representation as follows:

$$C_{t1} = G_1 a b^3 \quad C_{t2} = G_2 a b^3 \quad C_{t3} = G_3 a b^3 \quad . \quad (8)$$

The shear moduli for the principal directions of elasticity are denoted by $G_1(=C_{44})$, $G_2(=C_{55})$ and $G_3(=C_{66})$. Variables a and b are full sides of the rectangular section. The factor i is defined by the series as in the following equation (Lekhnitskii, 1977).

$$i = \frac{32d_i^2}{4} \quad \frac{1}{m^4} \left[1 - \frac{2d_i}{m} \tanh \frac{m}{2d_i} \right] \quad m=1,3,5, \quad (9)$$

where

$$d_1 = \frac{\frac{a}{b}}{\sqrt{\frac{G_1}{G_3}}} \quad d_2 = \frac{\frac{a}{b}}{\sqrt{\frac{G_2}{G_1}}} \quad d_3 = \frac{\frac{a}{b}}{\sqrt{\frac{G_3}{G_2}}} \quad . \quad (10)$$

The three natural frequencies observed via RUS for the split lowest mode correspond to three effective torsional rigidities. Thus, three equations based on Eq. 8 are sufficient to extract the three independent shear moduli of bovine bone as an orthotropic material. Eq. 10 were solved simultaneously for the shear moduli using commercial software "Mathematica" (Wolfram Research Inc, 100 Trade Center Drive, Champaign, IL 61820 Version 4.0) for numerical analysis. The upper limit for summation was increased until no significant change occurred in the result. It was observed that, from the sixth term on, there was no significant difference in the sum. Nevertheless, 100 terms were used to ensure convergence.

Transmission ultrasound

The ultrasonic test system utilizes a pulse generator (model: 500PR), 1 MHz and 10 MHz compression transducers, 1 MHz shear transducers (all Panametrics Co., Waltham, MA) and an oscilloscope (Leader model: LS 1020). The pulsed ultrasound was passed through the test specimen and sensed by an identical transducer at the opposite end. The zero time was set where the first maximum amplitude appeared with the two transducers in contact. A specimen was placed between the transducers and the time between zero and the next maximum amplitude was measured on the oscilloscope to determine the transmission time delay through the bone specimen. Compressional wave measurements yielded the elastic constants C_{11} , C_{22} and C_{33} in Eq. 2.

Tests to obtain the shear moduli were performed using ultrasonic shear transducers (1 MHz, Panametrics) as shown in Fig. 1 (a). The direction of shearing force was parallel to the BNC connector. Since bone samples are anisotropic, the measurement of shear moduli (C_{44} , C_{55} and C_{66} in Eq. 2) required proper the orientation of the specimen. These shear moduli from ultrasonic shear tests are compared with the shear moduli from RUS experiment in the following section.

IV. RESULTS

The RUS spectrum obtained for the first wet bovine bone sample (for sample location and density see Fig. 3) over a frequency range from 50 kHz to 500 kHz is shown in Fig. 4. The expected torsional resonant frequency using the forward calculation was 183 kHz. The torsion peak was observed at 182 kHz and its damping was calculated to be 0.034. As described above, a peak at 100 kHz was attributed to wave transmission through the air around the specimen. System noise was observed around 150 kHz and 170 kHz. When this overlapped a resonant peak, the sharp noise data were masked off prior to Lorentzian curve fitting.

The inset of Fig. 4 is the expanded RUS spectrum of the torsion mode for bovine bone sample #1. The torsion mode peak is highlighted by a down arrow in the figure. $\tan \delta$ of that peak was obtained as 0.034 by using Lorentzian curve fitting. Bovine bone, being an anisotropic material, was expected to have three split peaks representing shear properties in the radial, circumferential and longitudinal directions. However, the resonances associated with the shear moduli C_{44} , C_{55} and C_{66} are too close to resolve as separate resonant peaks. As can be seen from Eq. 4, a 10% difference in G (typical of the shear anisotropy observed by others) will result in 5% difference in resonant frequency. However a change of this magnitude could only be observed if the resonant peaks are sufficiently narrow as would be the case in a low damping material. For bovine bone, $\tan \delta$ at ultrasonic frequency is much larger than that of most engineering materials, and also much larger than in most materials previously studied via RUS. Consequently, the resonant peaks are

broad, and they overlap. As the mid-shaft of the bovine femur (from sample #3 to #8, see Fig. 3) was approached, torsion peaks for each specimen were split as shown in Fig. 5. This suggests that one torsion mode was separated enough to be revealed by RUS, but the other two modes still overlapped resulting in a broadened peak in the RUS spectrum. From sample #9, located 29 cm from the distal end, the torsion peak went back to one peak. This trend of one peak continued in the rest of the bovine samples.

Fig. 6 shows the RUS spectrum of the rectangular bovine sample with a 20% ratio between the dimensions (7.03 x 5.72 x 4.55 mm). The rationale behind the use of a rectangular sample was to achieve sufficient anisotropy in the geometry (since the resonant frequencies are proportional to $1/L$ (Eq. 4)) to separate the torsional modes into three distinct peaks. The rectangular sample was prepared from bone located directly next to the #1 sample's original location. Damping values of each peak from the Lorentzian curve fit were calculated to be $\tan \delta = 0.098, 0.079$ and 0.031 . Calculation from Lekhnitskii's (anisotropic) equations (8-10) disclosed shear moduli of 6.54, 6.32 and 4.17 GPa. For comparison the effective shear modulus for the cubical #1 sample was 6 GPa, similar to the values obtained using the Lekhnitskii equations. As for mechanical damping of cube specimens, a map of effective damping disclosed values between 0.02 and 0.09, however these are not considered meaningful due to the overlapping of resonant peaks. These results imply rectangular samples would be better than the cubes since they allow the splitting of the three torsional resonances and therefore resolution of the three shear moduli and determination of damping.

The map in Fig. 7 of the effective shear moduli (G_{eff}) versus sample position suggests an increased stiffness in the mid part of the bone. The effective shear modulus is the superposition of two tensorial shear moduli. To interpret the variation of effective modulus, a polynomial curve fit ($Y = -0.009x^2 + 0.497x + 0.085$ with Y as modulus and x as position along the bone in centimeters) was found and presented as a solid line. The overall change in stiffness was suggestive of the hypothesis of increased stiffness in the mid-shaft of the bone. To obtain tensorial shear moduli from effective moduli, three independent resonant frequencies must be input to Lekhnitskii's anisotropic equation. This was not possible for the cubic specimens because the three torsion resonance peaks overlapped owing to broadening from the high damping of bone. Error estimates are about 2% for resonant frequency therefore 4% for modulus.

Tensor modulus values C_{ij} from the ultrasonic transmission tests are shown in Fig. 8 and Table 1. Moduli vary with position in a bone and among different bones to a sufficient extent that differences among different reports is not unexpected. Owing to the painstaking nature of transmission ultrasound studies, prior reports tend to deal with a single specimen or few specimens. For further comparison, the moduli for *dry* human cortical bone obtained by Yoon and Katz (1976) are $C_{11} = 23.4$ GPa, $C_{33} = 32.5$ GPa, $C_{44} = 8.71$ GPa, $C_{12} = 9.06$ GPa, $C_{13} = 8.11$ GPa. Dry

bone is known to be stiffer than wet bone. The overall pattern of highest axial modulus in the 3 (longitudinal) direction is common to all the results including the present ones. In bovine bone, the circumferential direction is the next stiffest, and the radial direction is the least stiff. Referring to Fig. 8, data points with squares represent shear moduli of the specimen and can be compared with the RUS results in Fig. 7. The data are qualitatively similar to the results from RUS. The general trend between the two data sets has the same concave down shape; the difference between the minimum and maximum moduli is about 4 GPa for both sets. However, polynomial curve fitting of ultrasonic transmission results ($Y = -0.015x^2 + 0.86x - 7.38$, $R=0.76$, where Y is the modulus, x is the position along the bone in centimeters, and R is the correlation coefficient) exhibited a sharper concave down shape than the fitting of RUS results ($Y = -0.009x^2 + 0.49x + 0.085$, $R=0.41$). Curve fits confirm the perception of a maximum and moreover they quantify the degree of scatter.

V. DISCUSSION

In an isotropic material, the torsional resonance mode is the first to appear as frequency is increased (Fig. 2). To evaluate the result for the torsion peak at 182 kHz, the ratio between the torsion mode and the next higher mode was analyzed. In isotropic polymethyl methacrylate (PMMA) cubes, the ratio between the first torsion mode and the next flexure mode was 1.38 (Lee and Lakes 2000). In bovine bone samples, the ratio between the 182 kHz peak and the next resonance frequency at 253 kHz was 1.39. Since bone is not an isotropic material, one cannot make a direct comparison between these two ratios. Even so, they can be used as a general guideline as to where the torsion mode should be. Using the same calculation procedure for the peak at 182 kHz, an effective shear modulus of 6 GPa was obtained, which is reasonable for bovine bone. Therefore, the peak at 182 kHz was attributed to torsion even though the amplitude is much smaller than other resonances. A similar condition was observed in the case of PMMA (Lee and Lakes 2000).

RUS and transmission ultrasound tests differ in several ways. First, the ultrasonic transmission tests were performed at 1 MHz for both axial and shear waves while RUS resonances were near 100 kHz. Since bone is a viscoelastic material, its material properties depend on frequency. However, classical theories of a viscoelastic continuum predict the stiffness to increase with frequency. A decrease is possible only in non-classical theories which incorporate micro-vibration of structural elements. Therefore, lower stiffness in transmission ultrasound tests compared with RUS tests, which was observed in this study, needs to be explained by causes other than viscoelastic dispersion (frequency dependence of modulus) in a continuum view. For example, difference in strain gradient direction and magnitude can markedly influence the apparent stiffness of bone. Specifically, torsion and bending rigidity depends on size in a non-classical way (Ascenzi et al. 1994). The apparent shear modulus of slender specimens exceeded that of whole bone by a

factor of about four. These size effects have been explained in a continuum view by Cosserat elasticity and in a structural view by the heterogeneity in stiffness in human bone as a fibrous composite and bovine bone as a laminated composite (Lakes, 1995). Since the RUS lowest mode involved torsion resonance while ultrasonic transmission testing involved wave propagation of the specimen, there is a strain gradient difference in the comparison of these methods. In view of observed gradient effects reported elsewhere, we cannot expect the moduli obtained by these different methods to be identical. Error estimates for the modulus are about 4% based on reproducibility tests. In view of the relatively low ultrasonic frequency used and the size of the samples, this is not unreasonable.

Results are consistent with the observation of Pope and Outwater (1974) of increased elastic modulus in the mid-diaphysis of bovine tibiae. A histological correlation for the increased stiffness in the middle of the bone might be expected, but no obvious change in histology was apparent.

VI. CONCLUSIONS

A map of the effective shear moduli (G_{eff}) versus sample position exhibited an increased stiffness in the middle of the bone, as was hypothesized. Tensor modulus values versus sample position were similar for the ultrasonic transmission tests and for RUS. RUS of cubical specimens was found not to be an effective tool for the study of damping and anisotropy of bone because of the overlapping resonant peaks due to high damping of bone at ultrasonic frequency. Use of rectangular samples rather than cubes in RUS allows determination of three shear moduli and three shear damping values. For future work, experiments using more rectangular specimens rather than cubes are recommended. Such studies may explore differences from age related mineralization, or differences in effects of diet or disease.

VII. REFERENCES

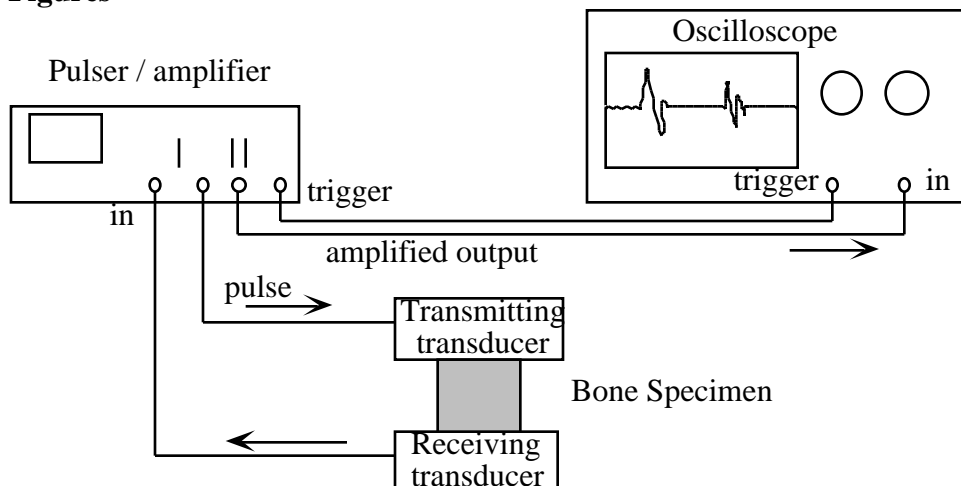
- Abendschein W, Hyatt G (1970) Ultrasonics and selected physical properties of bone. *Clinical Orthopedics and Related Research* 69: 294-301
- Andre M, Craven J, Greenfield M, Stern R (1980) Measurement of the velocity of ultrasound in the human femur in vivo. *Med Phys* 7(4): 324-330
- Ascenzi A, Baschieri P, Benvenuti A (1994) The torsional properties of selected single osteons. *J Biomech* 27: 875-884
- Brown S, Mayor M (1976) Ultrasonic assessment of early callus formation. *Biomed. Eng* 11: 124-136
- Demarest R (1971) Cube-resonance method to determine the elastic constants of solids. *J Acoust Soc Am* 49(3.2): 768-775
- Garner E, Lakes R, Lee T, Swan C, Brand R (2000) Viscoelastic dissipation in compact bone: implications for stress-induced fluid flow in bone. *J Biomech Eng* 122: 166-172
- Gere J, Timoshenko S (1990) *Mechanics of materials*. 3rd edition, PWS publishing, Boston
- Graesser E, Wong C (1992) *Mechanics and Mechanisms of Material Damping*. ASTM, Philadelphia
- Hamer A, Strachan J, Black M, Ibbtson C, Stockley I, Elson R (1996) Biomechanical properties of cortical allograft bone using a new method of bone strength measurement - A comparison of fresh, fresh-frozen and irradiated bone. *J Bone Joint Surg Br* 78B: 363-368
- Knets I (1978) *Mechanics of biological tissues*. *Polymer Mechanics* 13: 434-440
- Koppellmann V (1958) Uber die Bestimmung des dynamischen Elasticitatsmoduls und des dynamischen Schubmoduls im Frequenzbereich 10^{-5} bis 10^{-1} Hz. *Rheol Acta* 1: 20-28
- Lakes R, Saha S (1978) A noncontacting electromagnetic device for the determination of in vivo properties of bone. *Med Instr* 12(2): 106-109
- Lakes, R, Yoon, H. and Katz, J, (1983) Slow compressional wave propagation in wet human and bovine cortical bone, *Science*, 220: 513-515.
- Lakes R, Yoon H, Katz J (1986) Ultrasonic wave propagation and attenuation in wet bone. *J Biomed Eng* 8: 143-148
- Lakes, R (1995) On the torsional properties of single osteons, *J. Biomechanics*, 28: 1409-1410.
- Lakes R (1999) *Viscoelastic Solids*. CRC Press, Boca Raton, FL
- Lakes R (2001) Viscoelastic properties of cortical bone, *Bone Mechanics Handbook*, (ed. Cowin S) CRC Press, Second Edition, Boca Raton, FL
- Lang S (1970) Ultrasonic method for measuring elastic coefficients of bone and results on fresh and dried bovine bones. *IEEE Trans Biomed Eng* BME-17: 101-105

- Lee T, Lakes R (2000) Resonant ultrasound spectroscopy for measurement of mechanical damping: comparison with broadband viscoelastic spectroscopy. *Rev Sci Instr* 71(7) 2855-2861
- Lees S, Heeley J, Cleary P (1979) A study of some properties of a sample of bovine cortical bone using ultrasound. *Calcif. Tiss. Intern* 29:107-117
- Leisure R, Willis F (1997) Resonant ultrasound spectroscopy. *J Phys Cond Matter* 9: 6001-6029
- Lekhnitskii S (1977) Theory of elasticity of an anisotropic body. Mir publishers, Moscow
- Maharidge R (1984) Ultrasonic properties and microstructure of bovine bone and Haversian bovine bone modeling. Ph.D. Thesis, RPI
- Maynard J (1996) Resonant ultrasound spectroscopy. *Physics Today* 49: 26-31
- Migliori A, Sarrao J (1997) Resonant Ultrasound Spectroscopy, John Wiley, New York
- Papadakis E (1976) Ultrasonic velocity and attenuation: measurement methods with scientific and industrial applications, *Physical Acoustics*, (eds. Mason W and Thurston N) Academic Press, New York
- Pope, M. and Outwater, A. (1974) Mechanical properties of bone as a function of position and orientation *J. Biomechanics* 7: 61-66
- Sedlin E, Hirsch C (1966) Factors affecting the determination of the physical properties of femoral cortical bone. *ACTA Ortho Scand* 37(29) 29-48
- Van Buskirk W, Ashman R (1981) The elastic moduli of bone. *The Joint ASME-ASCE Conf.* 45: 131-143
- Yoon H, Katz J (1976) Ultrasonic wave propagation in human cortical bone. II Measurements of elastic properties and microhardness. *J Biomech* 9: 459-464

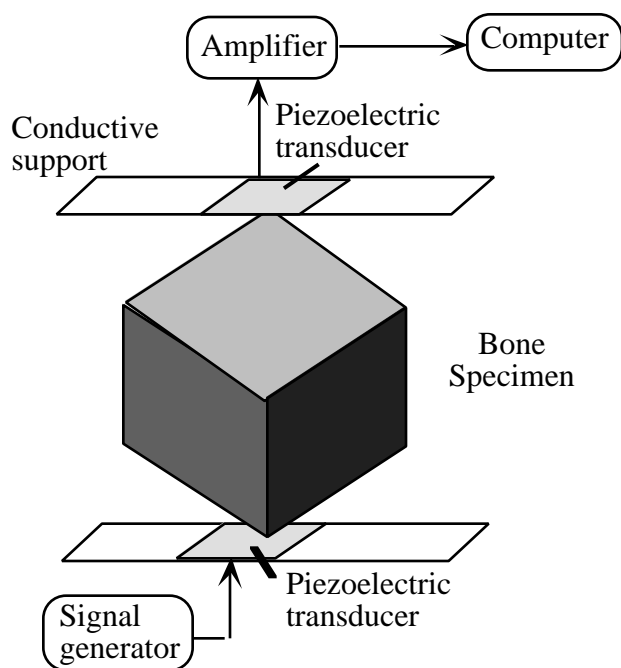
Tables

Table 1. Elastic stiffness coefficients from various bovine bones. All measurement made with transmission ultrasonic transducers (All values in GPa).

Figures



(a) Wave transmission ultrasound



(b) Resonant ultrasound spectroscopy (RUS)

Fig. 1 (a) Schematic diagram of through-transmission ultrasonic testing equipment.

(b) Schematic diagram of RUS (Resonant Ultrasound Spectroscopy) apparatus (adapted from Lakes 1998).

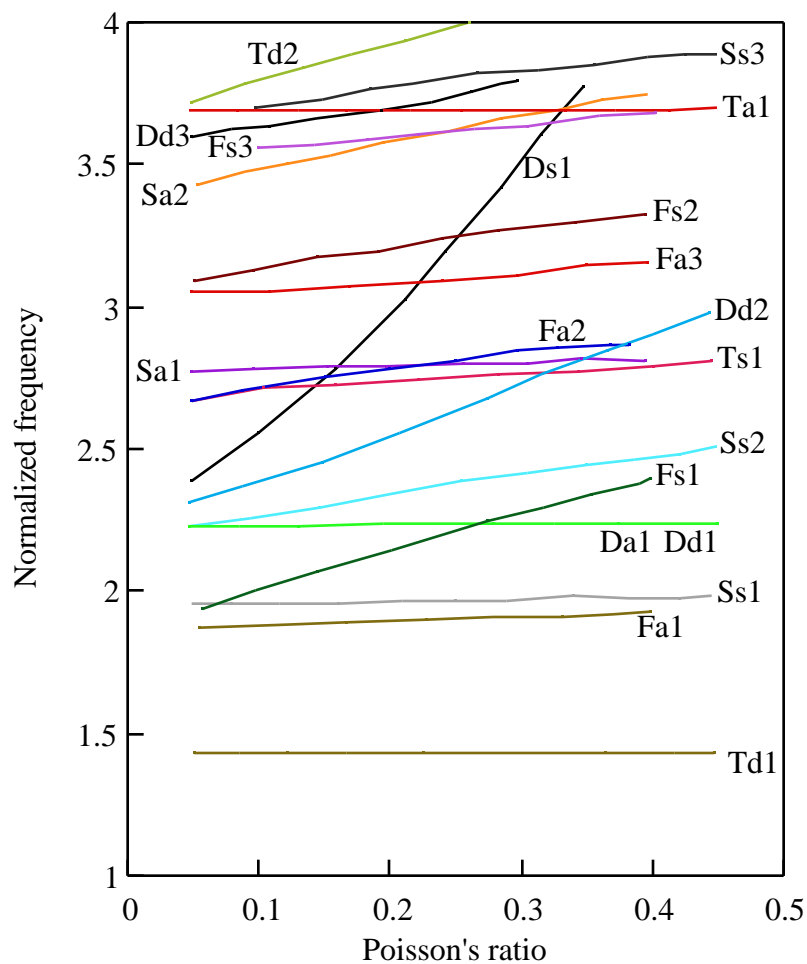


Fig. 2 Normalized theoretical resonant frequencies of an isotropic cube as a function of Poisson's ratio [adapted from Demarest 1971], for use in RUS studies. The lowest mode (Td1) is torsion. D refers to dilation, T to torsion, S to shear, and F to flexure. Subscript symbols are a, antisymmetric; s, symmetric; d, doublet. The integer subscripts order the modes by ascending frequency.

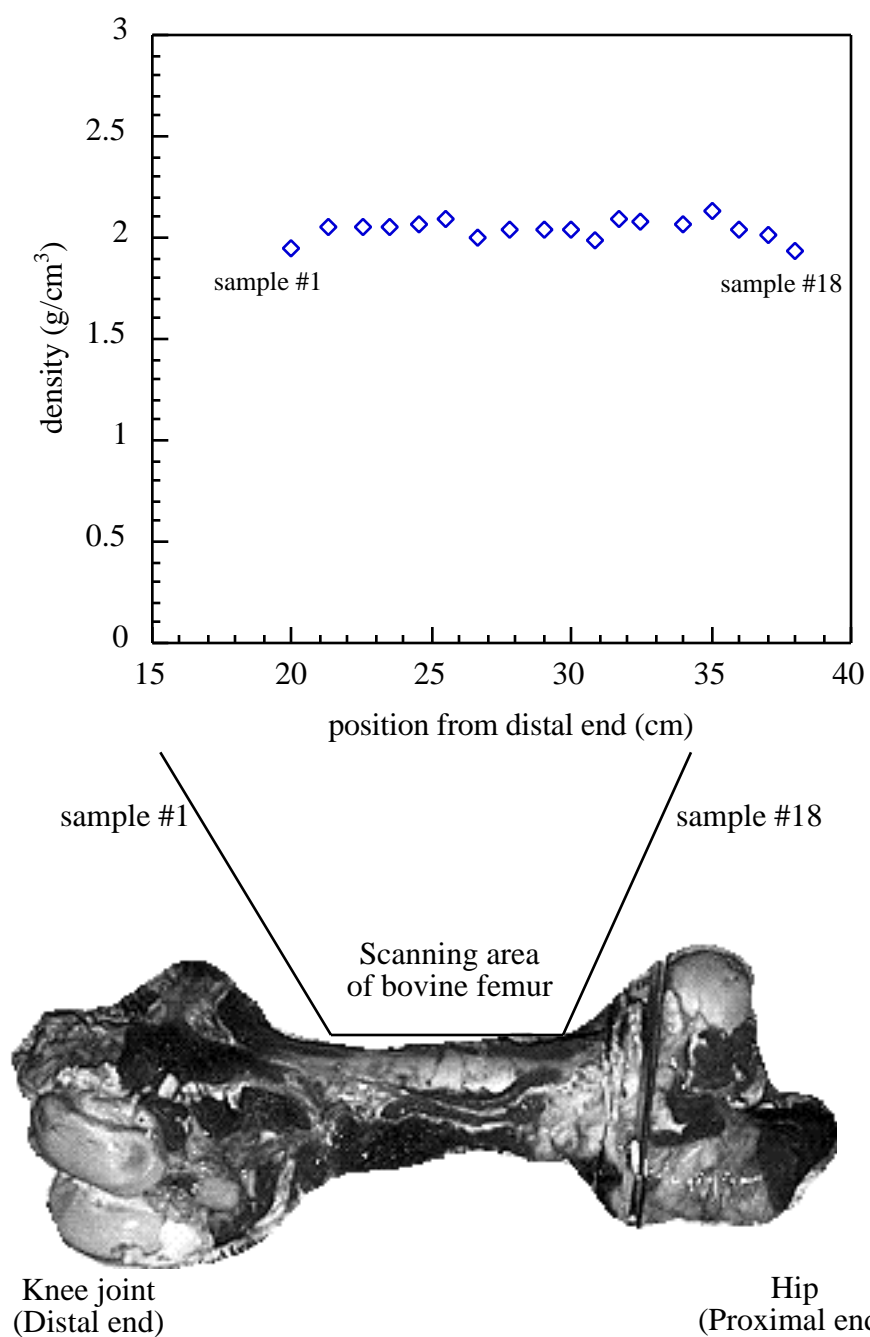


Fig. 3 Density versus position of eighteen wet bovine femur specimens and the testing area to the same scale.

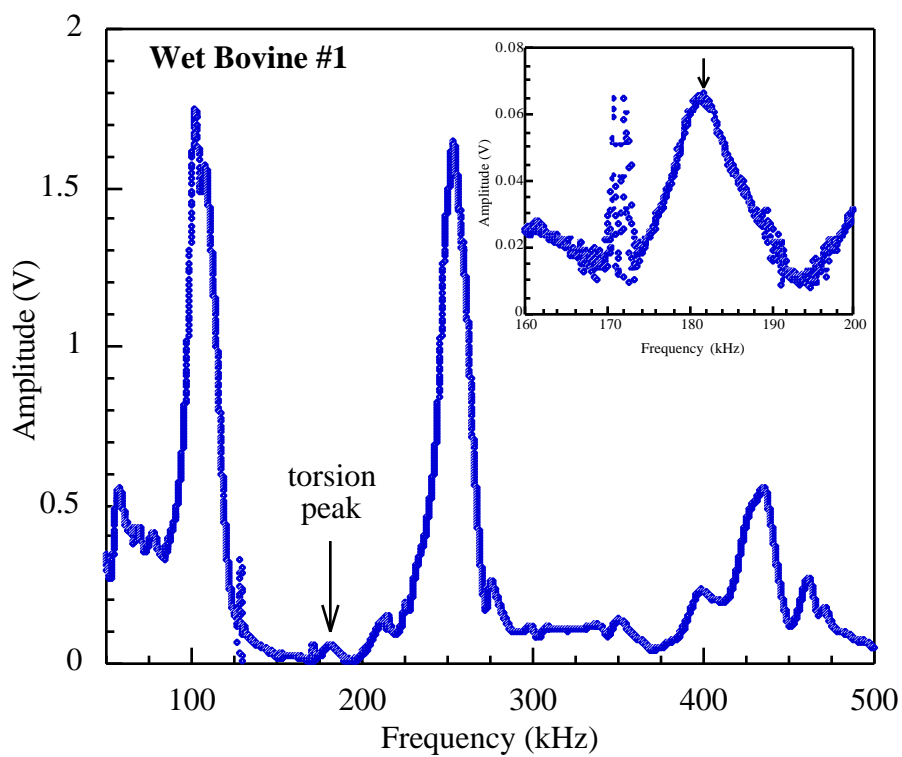


Fig. 4 RUS spectrum for bovine bone sample #1 with frequency range of 50 - 500 kHz. (Inset) spectrum of a torsion peak over a narrow range of frequency. Down arrow indicates torsion resonance.

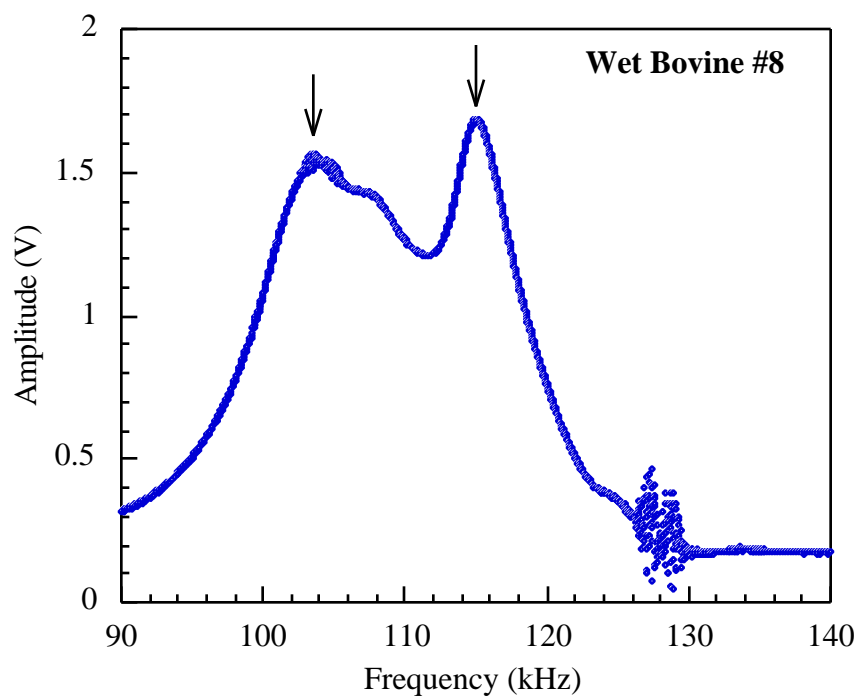


Fig. 5 RUS spectrum for bovine bone sample #8. System noise occurs around 127 kHz. Down arrows indicate resonant frequencies.

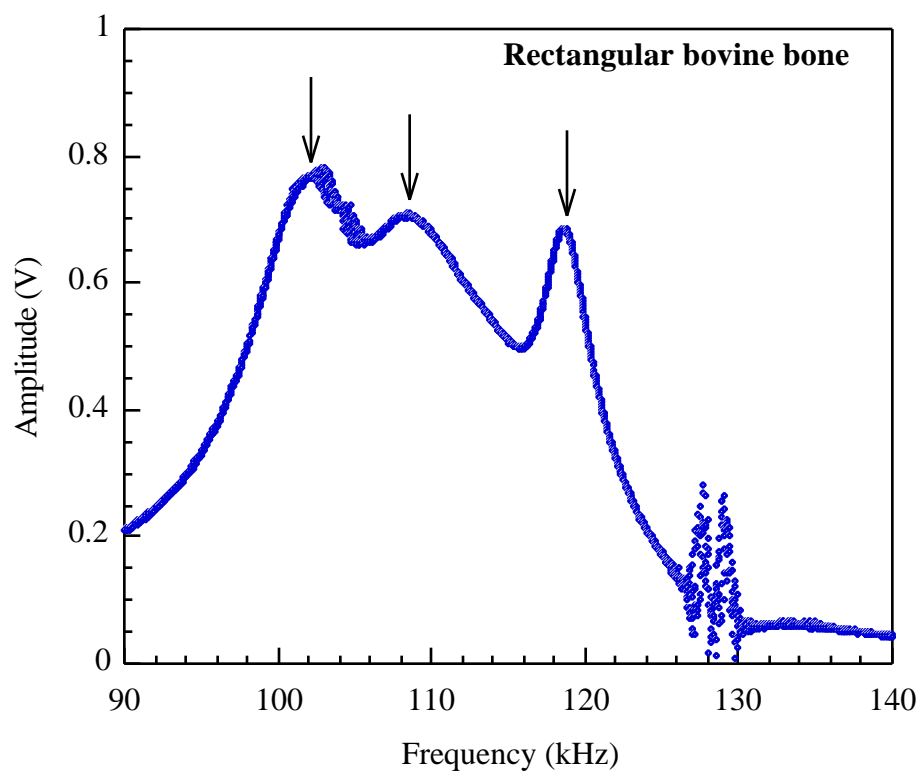


Fig. 6 RUS spectrum of a rectangular specimen of bovine bone. Down arrows indicate resonant frequencies.

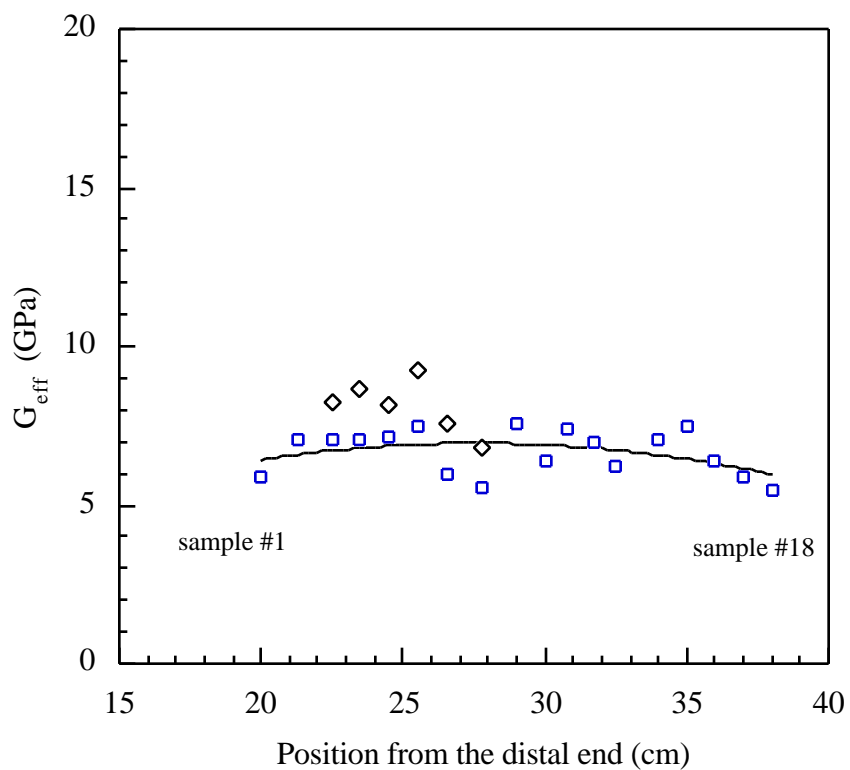


Fig. 7 Effective shear moduli from RUS versus sample position from the distal end. Squares represent moduli extracted from main peaks and diamonds represent moduli from secondary peaks observed from sample #3 to sample #8. Polynomial curve fitting ($Y=-0.009x^2+0.497x+0.085$, $R=0.41$) suggests a modest increase in modulus in the middle part of the bone.

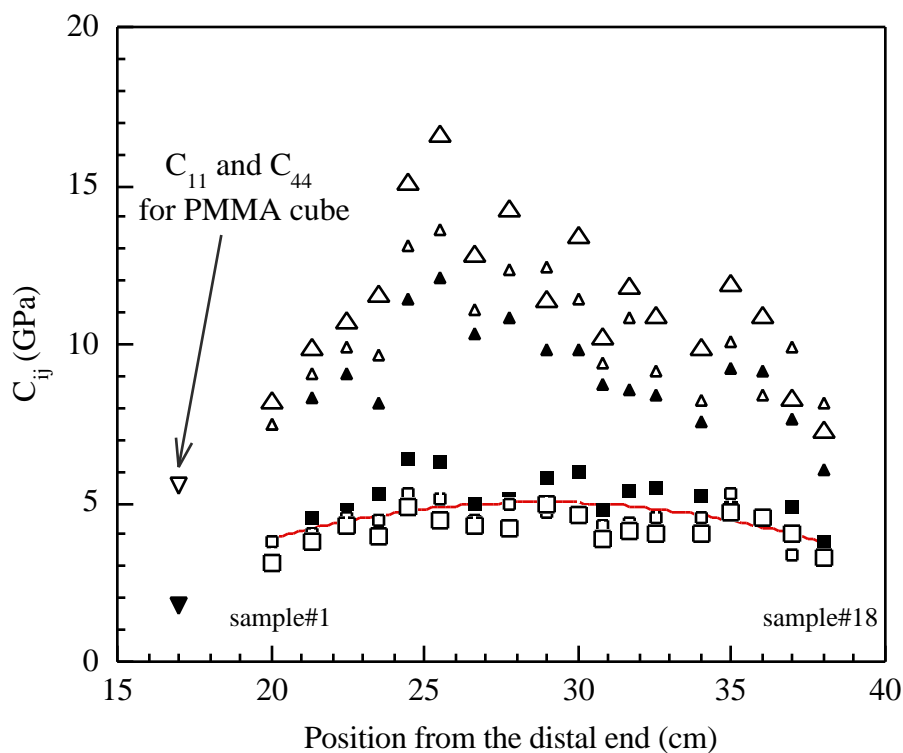


Fig. 8 Experimental results from ultrasonic transmission measurement of bovine bone. 1 MHz axial and shear transducers were used for measuring axial and shear stiffness. Small solid triangles, small open triangles and large open triangles represent axial moduli C_{11} , C_{22} and C_{33} , respectively. Small solid squares, small open squares, and open large squares represent shear moduli C_{44} , C_{55} and C_{66} , respectively. Polynomial curve fitting ($Y = -0.015x^2 + 0.86x - 7.38$, $R = 0.76$) suggests the modulus is higher in the middle part of the bone.

Table 1. Elastic stiffness coefficients from various bovine bones. All measurement made with ultrasonic transducers (All values in GPa).

Experimenters (Bone type)	C ₁₁	C ₂₂	C ₃₃	C ₄₄	C ₅₅	C ₆₆	C ₁₂	C ₁₃	C ₂₃
Van Buskirk (Bovine femur) ^a	14.1	18.4	25.0	7.0	6.3	5.28	6.34	4.84	6.94
Maharidge (Bovine femur Haversian) ^b	21.2	21.0	29.0	6.3	6.3	5.4	11.7	12.7	11.1
Maharidge (Bovine femur plexiform) ^c	22.4	25.0	35.0	8.2	7.1	6.1	14.0	15.8	13.6
Lang (Bovine phalanx) ^d	19.7	19.7	32.0	5.4	5.4	3.8	12.1	12.6	12.6
Present work (Bovine femur plexiform, wet) ^e	10.8	12.4	14.3	5.1	4.9	4.2	-	-	-

^a Frequency of both shear and longitudinal transducers: 2.5 MHz (Van Buskirk and Ashman 1981)

^{b c} Values from (Maharidge 1984)

^d Frequency of shear transducer was 2.25 MHz and longitudinal transducers was 5 MHz. Dry bone.

^e 1 MHz. Present work, wet, 28 cm from distal end, 7.15 mm cube, density 2.04 g/cm³. Off diagonal moduli were not measured.